Journal of Coastal Research	35	5	1095–1105	Coconut Creek, Florida	September 2019

www.JCRonline.org

TECHNICAL COMMUNICATIONS

www.cerf-jcr.org

Methodology for Identifying a Subset of Representative Storm Surge Hydrographs from a Coastal Storm Modeling Database

Dylan R. Sanderson*, Mark B. Gravens, and Rusty L. Permenter

Coastal and Hydraulics Laboratory
Engineer Research and Development Center
U.S. Army Corps of Engineers
Vicksburg, MS 39180, U.S.A.

ABSTRACT

Sanderson, D.R.; Gravens, M.B., and Permenter, R.L., 2019. Methodology for identifying a subset of representative storm surge hydrographs from a coastal storm modeling database. *Journal of Coastal Research,* 35(5), 1095–1105. Coconut Creek (Florida), ISSN 0749-0208.

Freely accessible databases that contain the results of large coastal storm modeling efforts are available online. Some of these databases explore coastal risks broadly (*e.g.*, overall vulnerability to sea-level rise and storm surge), whereas other databases contain more specific modeling results (*e.g.*, time series of storm surge hydrographs and associated significant wave heights). In the case of the latter, these databases can be composed of both synthetically defined, probabilistic storms as well as historically based storms. Some coastal storm modeling efforts have resulted in upwards of 1000+ simulated storm events. In the context of numerical models that use as input storm surge and significant wave height time series (*e.g.*, those that rely on precomputed relational databases), use of a full probabilistic storm suite can prove to be infeasible. A methodology for identifying a subset of representative storm events from a probabilistic database is outlined in this paper. By utilizing storm surge and significant wave height time series resulting from high-fidelity numerical modeling of the U.S. Army Corps of Engineers North Atlantic Coast Comprehensive Study, a representative storm suite was developed for Crisfield, Maryland. The results of using a representative storm suite and a full storm suite were compared by simulating 75 iterations (life cycles) of a 216-year period using the Monte Carlo life cycle model G2CRM. By performing a nonparametric extreme value analysis, the stage-frequency curves resulting from the representative and the full storm suites compared favorably.

ADDITIONAL INDEX WORDS: *Coastal hazards, probabilistic life cycle analysis, synthetic storm database.*

INTRODUCTION

Tropical cyclones are prevalent along the U.S. Gulf and East Coasts and pose a threat to coastal communities by inducing flooding, wave impact to structures, and, in the case of sandy beaches, erosion damages (FEMA, 2011; Hatzikyriakou and Lin, 2017, 2018; Rahmstorf, 2017). The general consensus among researchers is that the intensity of tropical cyclones will increase as the climate warms (Emanual, 2005; Sobel *et al.*, 2016; Webster *et al.*, 2005), with significant increases already observed over recent decades in the North Atlantic (Goldenberg *et al.*, 2001; Kossin, Olander, and Knapp, 2013; Walsh *et al.*, 2016).

To quantify the risks associated with potential tropical cyclones outside of the historical record, methodologies such as the Joint Probability Method (JPM; Myers, 1970) have been developed. JPM parameterizes historically observed data into a set of key forcing inputs (central pressure deficit, radius of maximum winds, translational speed, *etc.*). Each parameter corresponds to a probabilistic distribution, from which the JPM is implemented to define plausible storms outside of the historical record. Some older studies using the JPM have resulted in 3000+ simulated storm events (Toro *et al.*, 2010a).

To improve the computational efficiency and reduce the number of storms required to characterize the probabilistic space, optimal sampling methods within JPM (JPM-OS) have been proposed (Irish and Resio, 2013; Resio, 2007; Resio, Irish, and Cialone, 2009; Toro *et al.*, 2010a,b). Recent studies, such as the U.S. Army Corps of Engineers (USACE) North Atlantic Coast Comprehensive Study (NACCS; Nadal-Caraballo *et al.,* 2015), have used JPM-OS to parameterize tropical events, which then served as input to a planetary boundary layer model. Wind fields from the planetary boundary layer model output were then used to drive the high-fidelity storm surge and wind wave numerical models ADCIRC (Luettich, Westerink, and Scheffner, 1992) and STWAVE (Massey *et al.*, 2011). The NACCS study ultimately resulted in 1050 synthetic tropical storm events that characterize the coastal hazards from Virginia to Maine.

DOI: 10.2112/JCOASTRES-D-18-00052.1 received 18 April 2018; accepted in revision 25 January 2019; corrected proofs received 4 March 2019.

*Corresponding author: sandersondylan@gmail.com

Unlike tropical cyclones, extratropical cyclones cannot be easily parameterized; therefore, the JPM cannot be readily applied (Nadal-Caraballo *et al*., 2015). Where extratropical cyclones are prevalent (U.S. East Coast and Great Lakes), the probabilistic space is typically characterized by modeling historically observed storm events. Consequently, studies that characterize the risk associated with extratropical events often contain on the order of ~100 historically based storms.

Coastal Hazard Databases

Freely accessible databases are available online that store the results of coastal modeling efforts. The Nature Conservancy (2018) manages a Coastal Resilience program in which a mapping portal is available that allows users to visualize the risks associated with sea level rise and storm surge. Similarly, the U.S. Geological Survey (USGS, 2018) manages the Coastal Change Hazards Portal that explores extreme storm events, shoreline change and sea level rise.

Furthermore, USACE (2018) manages the Coastal Hazards System (CHS), which is an online database archive that contains storm surge hydrograph time series, wave time series, and relative probabilities of synthetic storm events resulting from comprehensive coastal studies. The CHS currently contains the results from multiple studies, including the NACCS, the Federal Emergency Management Agency Great Lakes Study (Nadal-Caraballo, Melby, and Ebersole, 2012), and the Sabine Pass to Galveston Study (Melby *et al*., 2017).

Goals

In this paper, a methodology of identifying a subset of representative storm events (12–36) from a probabilistic storm database is outlined. This methodology considers the storm surge hydrographs associated with both tropical and extratropical storm events. This methodology was originally developed for Beach-*fx,* where the model architecture necessitates a limited, representative storm suite (see below); however, other applications may be prevalent. The results indicate that identifying a representative storm suite using this methodology is a technically justifiable approach to limiting the number of storm events used in Monte Carlo life cycle modeling.

Probabilistic Life Cycle Analysis Modeling

Probabilistic Life Cycle Analysis (PLCA) models, such as Beach-*fx* (Gravens, Males, and Moser, 2007) and G2CRM (Generation 2 Coastal Risk Model; under development), are engineering-economic models that estimate a project's physical behavior and economic benefits including uncertainty over the project's expected life cycle. As input to these PLCA models, environmental forcing plays a key role and consists of storm surge hydrograph and wave time series. By implementing Monte Carlo methods, these models iterate over a project's life cycle hundreds of times, with each iteration involving a unique sequence and occurrence of storm events.

These PLCA models rely on prepopulated relational databases that are accessed at run time to obtain a project's response to the selected storm event. The Beach-*fx* relational database includes a matrix of prestorm beach profiles and storm events from which poststorm beach morphology changes are extracted. Because precomputed coastal responses are employed by the PLCA models at run time, the response database must be populated with responses appropriate for the range of prestorm upper beach states that may be encountered over the simulated life cycle. On the order of 200 unique upper beach profile configurations (variations in dune height, dune width, and berm width) are necessary to capture the expected range of prestorm conditions for a single beach profile, or reach. Within Beach-*fx*, there may be between three and nine representative reaches in a study, thus increasing the number of prestorm profiles to 600–1800. Furthermore, each storm surge hydrograph is combined with 12 representations of the astronomical tide to cover variations in tidal range and phasing of the storm surge hydrograph with the tide signal. A typical probabilistic storm database may have upwards of 500 relevant synthetic storm events. Considering the necessary permutations, the number of profile/response combinations (*i.e*. the number of storm response simulations required) quickly becomes untenable, jumping to approximately 3.6–10.8 million. One method to reduce the number of profile/response combinations is to reduce the number of unique storm events while still capturing the probabilistic space of the local storm climatology.

Study Area—Crisfield, Maryland

Crisfield, Maryland, is located on the Chesapeake Bay (Figure 1) and is subject to surge-induced flooding from both tropical and extratropical cyclones (Canick, Carlozo, and Foster, 2016). The combination of tides, sea level rise, and storm-induced inundation make Crisfield particularly vulnerable to coastal hazards. Given the environmental forcing conditions present at Crisfield, this site was identified as suitable to develop a representative storm suite.

CHS ADCIRC save point 6125 (STWAVE save point 507) is located near Crisfield (Figure 1). At the selected save point, 1050 synthetic tropical storm events and 100 extratropical storm events were obtained from the CHS. The storm surge and significant wave height time series were extracted. The methodology proposed in this paper to select representative storm events is generalized enough to be applied to areas not located along the North Atlantic Coast.

METHODS

At the selected save point, both tropical and extratropical storm events were considered. Because the methodologies used to generate the storm events differ (probabilistic *vs*. historic), the methods of selecting representative storms slightly diverge.

The general methodology used to develop a representative storm suite can be broken into five steps: (1) identification of storms of interest; (2) grouping of storms into clusters by the magnitude of the peak surge generated; (3) further subdividing storm clusters, if appropriate, by duration of storm surge hydrograph or range of peak amplitudes; (4) selection of representative storm events within each storm (sub)cluster; and (5) assigning appropriate relative probabilities to each selected representative storm. Unless otherwise specified, the methods implemented were equivalent for both tropical and extratropical events.

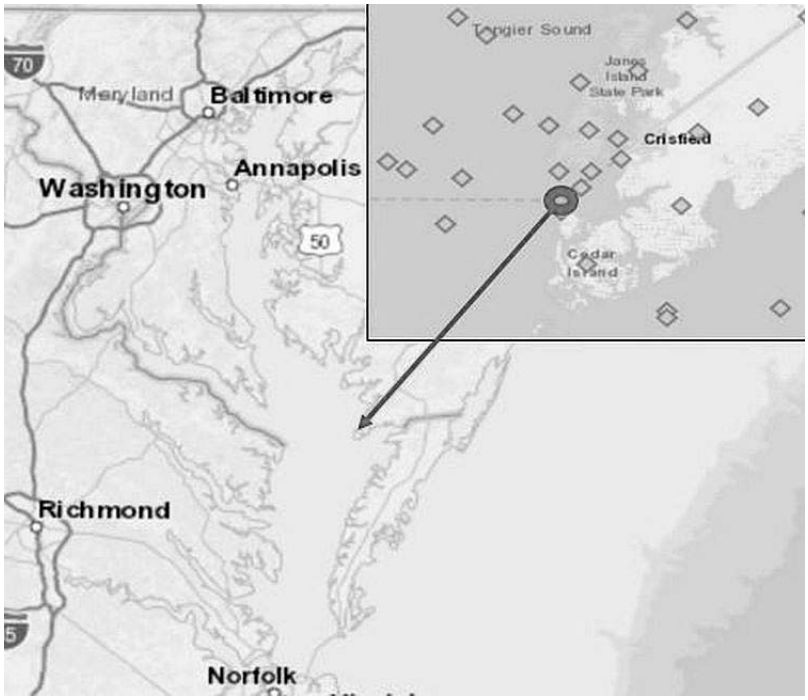

Figure 1. Location of Crisfield, Maryland, within the Chesapeake Bay. CHS ADCIRC station 6125 (STWAVE 507) is shown with the red circle. (Color for this figure is available in the online version of this paper.)

Identification of Storms of Interest

The CHS provides a unique estimate of relevant tropical storms occurrence rate for both low- and high-intensity storms as part of the attribute information for each save point in the database (Nadal-Caraballo *et al*., 2015). The storm occurrence rates provided on the CHS are a function of the radius around the study area used to define storms of interest. By performing a series of sensitivity analyses with radii ranging from 100 to 500 km, Nadal-Caraballo *et al*. (2015) implemented the Gaussian Kernel Function method (Chouinard and Liu, 1997) to determine an optimal kernel size of 200 km. Therefore, for consistency with their study, only those storms whose track passed within a 200-km radius of the study area were considered relevant to the local storm climatology. Use of a 200-km radius is arbitrary, and other radii may be selected, because the radius will consequently affect storm occurrence rates.

The storm occurrence rate becomes input to the PLCA tools and is used to dictate how often storm events are sampled within the Monte Carlo simulation. This step of isolating the locally relevant tropical storms for the Crisfield project site resulted in a reduction of available storms from 1050 to 415 (Figure 2).

The extratropical storms of interest were defined as those that were considered damage-producing. To isolate the damage-producing storms, a peak-over-threshold analysis of the peak surge generated for each storm event was performed (threshold value of 0.5 m). Storms with a peak surge less than 0.5 m were not considered damage-producing events in the context of the Crisfield project site. This step reduced the available extratropical storms at Crisfield from 100 to 90.

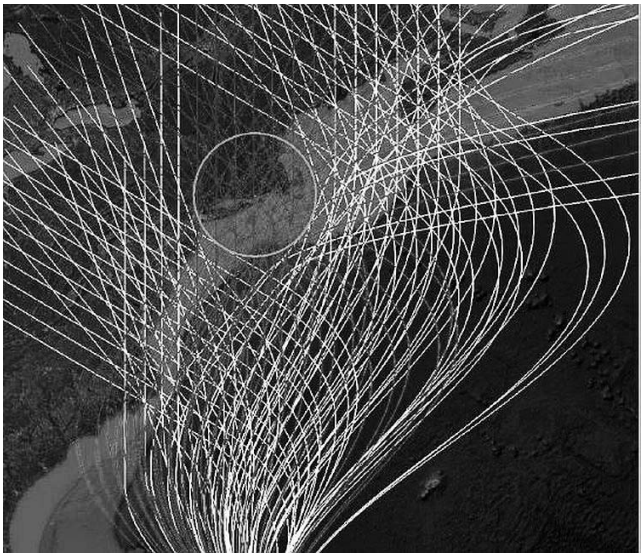

Figure 2. Storms whose storm tracks passed within the 200-km radius (red) around Crisfield, Maryland, were considered for further analysis. All other storm tracks (white) were considered irrelevant to local storm climatology. (Color for this figure is available in the online version of this paper.)

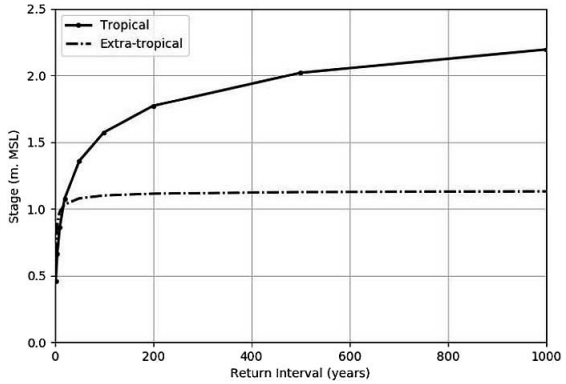

Figure 3. Annual exceedance probability for NACCS ADCIRC save point 6125. Tropical storms (solid) and extratropical (dash-dot) hazard curves are shown. The hazard curves were used to generate the storm cluster upper and lower limits.

Grouping of Storms into Clusters

The storms of interest were then grouped into clusters by the peak surge generated. The clusters were defined using the annual exceedance probability (AEP) curves available on the CHS at the selected save point (Figure 3). The CHS provides AEP curves in the form of stage values at specific predefined return interval years (2, 5, 10, 20, 50 y, *etc*.). Additionally, AEP curves are available for tropical storms, extratropical storms, or the two combined.

In this case, the tropical and extratropical storms were considered separately; therefore, tropical storm clustering relied on the tropical AEP curve, and the extratropical storm clustering relied on the extratropical AEP curve. For each available return interval year, a cluster was created (2-y cluster, 5-y cluster, *etc*.). The lower and upper limits of each cluster were specified as the midpoint between the clusters' nearest neighbors. For example, the lower limit of the 20-year cluster was defined as the midpoint between the surge values associated with the 10- and 20-year return intervals. Likewise, the upper cluster limit was defined as the midpoint between the surge values associated with the 20- and 50-year return intervals. At the lowest return interval (2-y) the lower cluster limit was defined as 0.5 m because storms that produce a peak surge less than 0.5 m are not damage producing at the example study area. Table 1 shows the CHS tropical storm AEP curve, and Table 2 shows the tropical storms' lower and upper cluster limits.

Each storm was then assigned to a cluster by isolating the peak surge elevation and combining it with a statistically defined mean high tide amplitude. The estimated mean high tide amplitude was added to the storm surge hydrographs because the AEP curve selected to group the storms into clusters included a tidal contribution. The mean high tide amplitude was computed by analyzing a 19-year-long tidal epoch at the study area.

Of the 415 tropical storms, 60 storms had a peak surge of less than 0.5 m and were not considered for further analysis. The remaining 355 storms were grouped into nine clusters. The 90 extratropical storms were grouped into six clusters.

Table 1. *Tropical AEP curve provided by CHS and resulting storm clusters.*

Return Year	Stage (m)
1	—
2	0.73
5	0.89
10	1.04
20	1.22
50	1.49
100	1.68
200	1.88
500	2.13
1000	2.30
2000	2.46
5000	2.64
10,000	2.77

Subdivision of Clusters

In the majority of the resulting clusters, particularly those with a large number of storms (high-frequency storm events), noticeable populations of both short/long duration storms and low/high amplitude storms were apparent. In these cases, the clusters were further divided to represent the various groupings present. For example, if a cluster had a significant population of short- and long-duration storms, then two clusters, or subclusters, were set up to distinguish between the two populations. Figure 4 shows an example of the 50-year return interval cluster. Before the peak surge, a notable separation between the long- and short-duration storm surge hydrographs can be seen.

The nine tropical clusters were divided into a total of 22 subclusters, representing short- and long-duration subclusters, as well as low, medium, and high peak amplitude subclusters. The six extratropical clusters were further divided into 10 subclusters. The number of subclusters present within each cluster can be seen in Table 3.

Selection of Representative Storms

After division of clusters into subclusters (if applicable), one representative storm surge hydrograph for each (sub)cluster was selected. The representative storm surge hydrographs were manually chosen such that the peak amplitude and duration both reasonably characterize the collection of storms

Table 2. *Tropical storm cluster limits.*

Lower Cluster Limit (m)	Return Interval Year (cluster no.)	Upper Cluster Limit (m)
0.5	2 (1)	0.81
0.81	5 (2)	0.96
0.96	10 (3)	1.13
1.13	20 (4)	1.35
1.35	50 (5)	1.59
1.59	100 (6)	1.78
1.78	200 (7)	2.01
2.01	500 (8)	2.21
2.21	1000 (9)	2.38
2.38	2000 (10)	2.55
2.55	5000 (11)	2.70
2.70	10,000 (12)	—

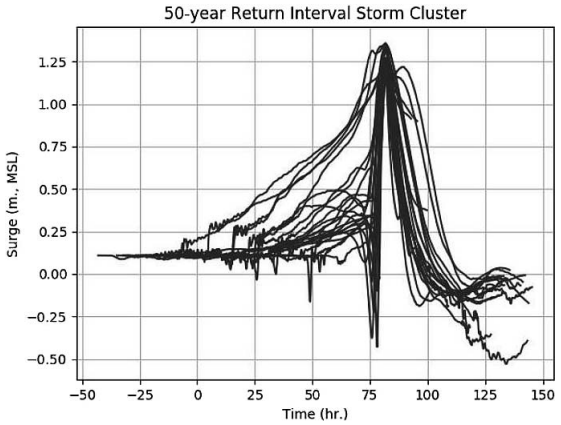

Figure 4. Example of the 50-y return interval tropical storm cluster. Note the separation between long- and short-duration storms.

in their respective (sub)cluster. For example, a representative storm would have both a peak surge amplitude and duration near the mean of all storms in the cluster. Figure 5 shows an example of the representative storms identified for the subclusters corresponding to a 50-year return interval stage. A total of 32 representative storms (22 tropical; 10 extratropical) were selected. The selected representative storms can be seen in Table 3.

Assignment of Relative Probabilities

The representative storms were then each assigned a relative probability of occurrence. The CHS provides storm-specific relative probabilities defined by the JPM integral of the storm characteristics, such as track location, heading direction, central pressure deficit, radius of maximum winds, and translational speed (Nadal-Caraballo *et al*., 2015).

The relative probabilities of the representative storms were computed by summing the relative probabilities of the storms being represented; that is, if a cluster (or subcluster) contains 20 storm surge hydrographs and is represented by a single representative storm surge hydrograph, then the relative probability assigned to the representative storm is equal to the sum of the relative probabilities of the 20 storms being represented. Table 3 shows a summary of the results of the selection process, including each (sub)cluster, the selected representative storm, the relative probability, and the number of storms being represented.

Assignment of Storm Rates

Storm rates dictate how often storm events are sampled in the PLCA models. The CHS provides spatially dependent storm recurrence rates at each save point for the synthetically defined storms (storms/y per km). The storm recurrence rates developed for the NACCS study were defined by a Gaussian Kernel Function (Nadal-Caraballo *et al*., 2015). Because a 200-km radius was used to generate a subset of storms, the CHS storm recurrence rates were multiplied by 400 (diameter in kilometers), resulting in storm occurrence rates in storms per year. The annual storm occurrence rate was distributed across the tropical storm season as defined by the NACCS study

Table 3. *Selected representative tropical and extratropical storms.*

Storm Type	Cluster No.	Representative Storm ID	Relative Probability	No. of Storms Represented	Note†
Tropical	1	240	0.0364289	33	1
Tropical	1	393	0.0384474	40	2
Tropical	1	647	0.0469166	62	3
Tropical	2	198	0.001504	10	4
Tropical	2	180	0.011526	18	6
Tropical	2	473	0.011526	18	7
Tropical	2	1007	0.011526	18	8
Tropical	3	277	0.0049432	12	4
Tropical	3	314	0.0090688	14	6
Tropical	3	174	0.0097165	15	7
Tropical	3	92	0.0097165	15	8
Tropical	4	315	0.0027349	9	4
Tropical	4	136	0.0186826	35	5
Tropical	5	195	0.000363	5	4
Tropical	5	278	0.0124107	20	5
Tropical	6	284	0.0006979	8	4
Tropical	6	524	0.004139	10	5
Tropical	7	107	0.0000612	1	4
Tropical	7	114	0.0025322	7	5
Tropical	8	271	0.0000775	1	4
Tropical	8	625	0.00047	2	5
Tropical	9	623	0.000636	2	—
Extratropical	1	92	0.1000	9	—
Extratropical	2	26	0.1778	16	1
Extratropical	2	47	0.1333	12	2
Extratropical	2	5	0.1222	11	3
Extratropical	3	83	0.1556	14	1
Extratropical	3	15	0.1111	10	3
Extratropical	4	29	0.0556	5	4
Extratropical	4	20	0.0556	5	5
Extratropical	5	1	0.0556	5	—
Extratropical	6	60	0.0333	3	—

†*1 = low-amplitude storms; 2 = mean-amplitude storms; 3 = high-amplitude storms; 4 = long-duration storms; 5 = short-duration storms; 6 = short-duration, low-amplitude storms; 7 = short-duration, mean-amplitude storms; 8 = short-duration, high-amplitude storms*

(Cialone *et al*., 2015) (June, 0.04; July, 0.04; August, 0.26; September, 0.48; October, 0.12; November, 0.06). These weights provided the storm occurrence rate on a monthly basis for the tropical storm season.

Because the extratropical storms were selected from a historic record, the storm occurrence rates were computed based on the observed events. The total number of extratropical storms under consideration (90) was divided by the number of years the historical record spanned (75), resulting in a storm occurrence rate of 1.2 storms/y. These storm occurrence rates were uniformly distributed across the extratropical storm season (October–March). The storm occurrence rates for both tropical and extratropical storms by month are shown in Table 4.

G2CRM Model Runs

The outlined procedure resulted in 32 storms (22 tropical; 10 extratropical) that are representative of the 445 damage-producing storms (355 tropical; 90 extratropical). To validate the use of the representative storm suite, two G2CRM simulations were performed in which one had access to the selected 32 representative storms and the other access to the 445 storms that were identified as locally relevant to the study area. G2CRM was selected for use because precomputed

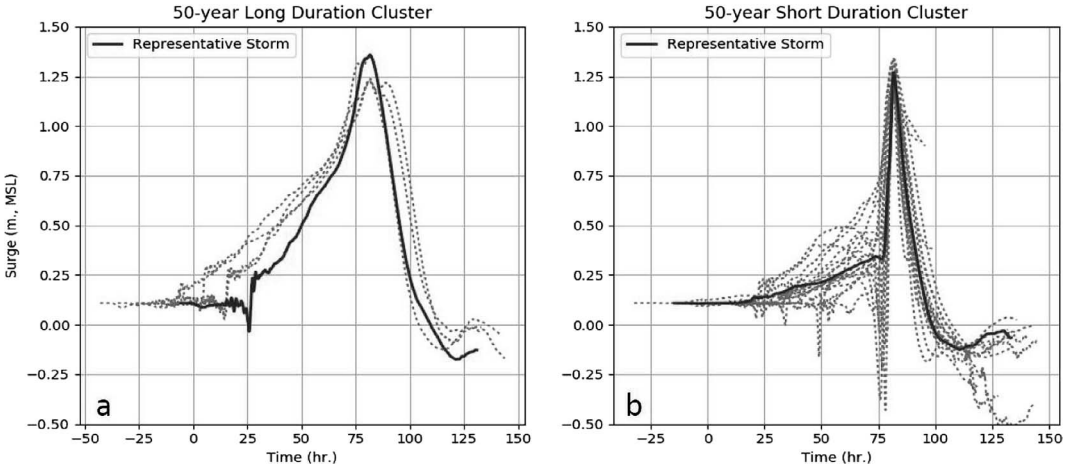

Figure 5. Example of 50-y return interval of (a) long- and (b) short-duration subclusters. The selected representative storms are highlighted and characterize their respective subcluster. (Color for this figure is available in the online version of this paper.)

databases (as in Beach-*fx*) are not necessary for run time. The emphasis for the model runs is on the occurrence and order of storm events rather than the results of the model. Because both Beach-*fx* and G2CRM use the same procedure to select storm events, it is technically justifiable to use G2CRM to validate the representative storm suite, although use of a representative storm suite is not a necessity for G2CRM.

G2CRM internally computes tidal elevation time series based on the identification of a tide save point. At the occurrence of a storm event within a simulation, the tide time series is computed and combined with the storm surge hydrograph to compute the total water elevation.

The goal of this validation effort is to demonstrate that the use of a representative storm suite will effectively return the same mean stage frequency relationship as is obtained when the full storm suite is used at a fraction of the computational effort. To achieve this end, G2CRM was configured to simulate 75 iterations of a 216-year life cycle. This setup allows for the estimation of a stage-frequency curve (out to the 216-y return interval) for each of the simulated life cycles using nonparametric extreme value analysis techniques. Incidentally, this setup (75 iterations of a 216-y life cycle) is, in some sense, consistent with typical project applications of PLCA model simulations, which commonly involve the simulation of 300 iterations of a 54-year life cycle. In both cases 16,200 total years are simulated.

Table 4. *Storm occurrence rates.*

Month	Tropical (storms/y)	Extratropical (storms/y)
Jan	0	0.2
Feb	0	0.2
Mar	0	0.2
Apr	0	0
May	0	0
Jun	0.007952	0
Jul	0.007952	0
Aug	0.051688	0
Sep	0.095424	0
Oct	0.023856	0.2
Nov	0.119280	0.2
Dec	0	0.2

In both simulations—representative storm suite and full storm suite—G2CRM sampled randomly from the available storms according to the specified storm occurrence rate and each storm's relative probability. The storm occurrence rate determines when in each life cycle a storm event occurs (Table 4), whereas each storm's relative probability dictates which storm occurs (Table 3). Because the storm occurrence rates were the same for both the representative and full storm suites, G2CRM returned the same number of storm events in each simulation. Both the representative and full storm suites have the same model run times (approximately 1 h).

RESULTS

By treating each storm event as an observation and extracting the annual peak stage (surge plus random tide), a nonparametric extreme value analysis was used to generate a stage-frequency curve for each life cycle (Scheffner *et al.*, 1999). Through this method, a cumulative distribution function (CDF) was estimated empirically and given by the relationship:

$$F_x(x_r) = \frac{r}{(n_{obs} + 1)} \quad (1)$$

where, $F_x(x_r)$ is the empirical estimate of the CDF, x_r is the rank ordered stage elevation (smallest to largest), n_{obs} is the number of observations, and r is the rank (1 through n_{obs}). From Scheffner *et al.* (1999), this form of the CDF estimate allows for values of the resulting stage-frequency curve to fall outside the smallest and largest observed values ($n_{obs} + 1$ in the denominator).

The annual probability of nonexceedance corresponding to an n-year return period event is given by:

$$F(x_n) = 1 - \frac{1}{n} \quad (2)$$

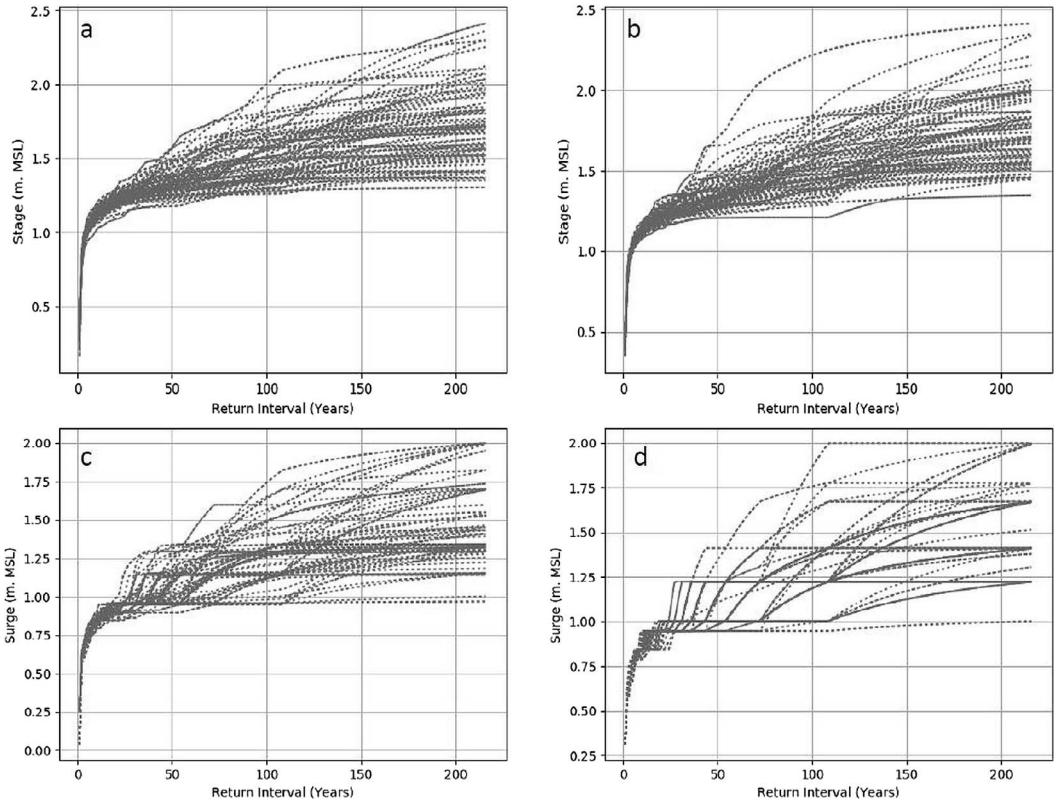

Figure 6. Hazard curves resulting from 75 iterations of a 216-y life cycle. Shown are: (a) stage of full storm suite, (b) stage of representative storm suite, (c) surge of full storm suite, and (d) surge of representative storm suite.

Therefore, the n-year return period stage value is obtained by computing $F(x_n)$ and linearly interpolating the stage value from $F_x(x_r)$.

Because of the variability in each life cycle, some simulated years did not experience storm events. In the case of no "recorded" storm event, the largest tide value associated with the life cycle under consideration was taken as the annual maximum. Through the use of Equations (1) and (2), the stage-frequency curve associated with each life cycle was computed. This resulted in two sets of 75 stage-frequency curves (representative and full storm suite) that span return intervals from 1 to 216 years (Figure 6a,b). In addition to the stage-frequency curves, the tidal contribution to stage was removed, and surge-frequency curves were generated (Figure 6c,d). For all sets of hazard curves in Figure 6, the mean was computed at each return interval year (Figure 7; black and red).

Although the selection of a representative storm suite considered only the storm surge hydrograph time series, coincident significant wave height time series associated with each storm event were evaluated through use of Equations (1) and (2). Similar to the computation of the stage-frequency curves, only the peak value associated with each significant wave height time series were considered. In addition to stage and surge, Figure 7 shows the resulting mean significant wave height–frequency curves for both the representative and full storm suites (blue).

Figure 7 shows that the average hazard curves for the representative storm suite compare favorably with those of the full storm suite. The stage, surge, and significant wave height–frequency curves all show the largest disparity in the higher return interval years. These differences are approximately 0.03, 0.05, and 0.02 m for stage, surge, and significant wave height, respectively.

DISCUSSION

The methodology outlined in this paper results in a technically justifiable approach of identifying representative storm events from a full probabilistic storm database. By simulating 75 iterations of a 216-year life cycle, 75 stage-frequency curves were generated for both the representative and full storm suites. The stage (surge plus tide), surge only, and significant wave height were considered for the hazard analysis. Although the mean significant wave height curves compare favorably, the selection process was based on the storm surge hydrograph time series, and not the wave time series. Consequently, the discussion focuses only on stage and surge.

Distribution of Stage-Frequency Curves

From Figure 6c,d, it can be seen that when considering only storm surge with no tide contribution, the distribution of stage-

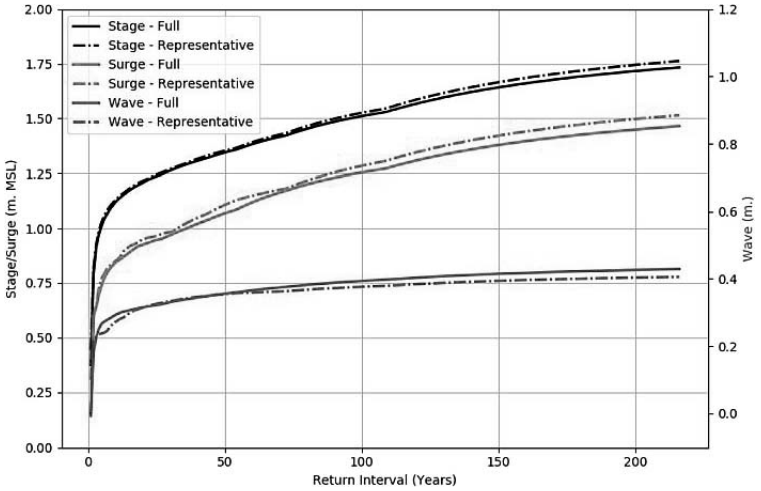

Figure 7. Averaged annual exceedance hazard curves corresponding to stage (black), surge (red), and significant wave height (blue). The full storm suite (solid) and representative storm suites (dash-dot) are shown. (Color for this figure is available in the online version of this paper.)

frequency curves becomes more discrete (Figure 6d). Although it appears that there are fewer hazard curves in Figure 6d, this is not the case, because of multiple identical curves. The discrete nature of the surge-frequency curves is expected because the phasing of tidal contribution in G2CRM is random, thus introducing more variability in the total water elevations that were used to compute the hazard curves; that is, the surge-frequency curves of Figure 6d were generated from 32 storm events, or 32 distinct peak water elevations. In the presence of tides, the 32 distinct peak water elevations become "infinite" within some range, because the phasing of the tide time series with the storm surge hydrograph time series is random.

To compare the variation in the distribution of stage-frequency curves across all return interval years, the standard deviation of each distribution was considered. From Figure 6, it can be seen that each G2CRM model simulation resulted in a distribution of 75 stage- and surge-frequency curves that span $\{n = 1, 2, 3, \ldots, 216\}$. By treating each n-year distribution independently, the standard deviation was computed for both the representative and full storm suites. Plots of the standard deviation at each return interval year can be seen in Figure 8.

From Figure 6, it can be seen that as the return interval year increases, the distribution of stage-frequency curves likewise increases. This is shown in Figure 8, with the increased standard deviation. The increase in standard deviation with the return interval year is attributed to the occurrence of low- *vs*. high-frequency storm events. Because the probability of occurrence associated with low-frequency (high-magnitude) storm events is lower than that of high-frequency storms, the low-frequency events were not sampled as often in the Monte Carlo life cycle simulation. Therefore, some iterations do not sample any low-frequency storm events, resulting in the lower stage-frequency curves of Figure 6. Conversely, some iterations do sample low-frequency storm events (possibly more than once) and are reflected by the upper stage-frequency curves in Figure 6. The high-frequency (low-magnitude) storm events associated with the lower return interval years are typically sampled repeatedly throughout each life cycle, ultimately resulting in less variability.

Figure 8 additionally shows that the standard deviation associated with the stage (black curves) begins to show disparities at the higher return interval years. It can be seen that between return interval years 1 and 108, the standard deviation of the distributions are nearly identical. Beyond the 108 return interval year, the standard deviations begin to diverge; however, the differences are relatively minor (approximately 0.03 m). This trend is attributed to the tidal contribution to total stage.

In both G2CRM model runs (full and representative storm suites), the timing of storm events within a life cycle are identical, although the selected storms are different. Because

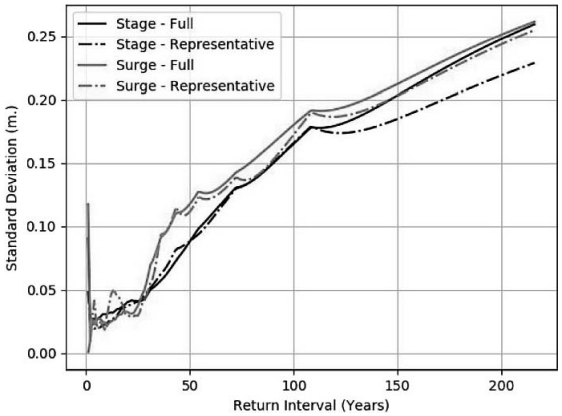

Figure 8. Standard deviation *vs*. return interval year for both stage (black) and surge (red). The full storm suite (solid) and representative storm suites (dash-dot) are shown. Note the separation in the standard deviation of stage (black) beyond the 108 return interval year. (Color for this figure is available in the online version of this paper.)

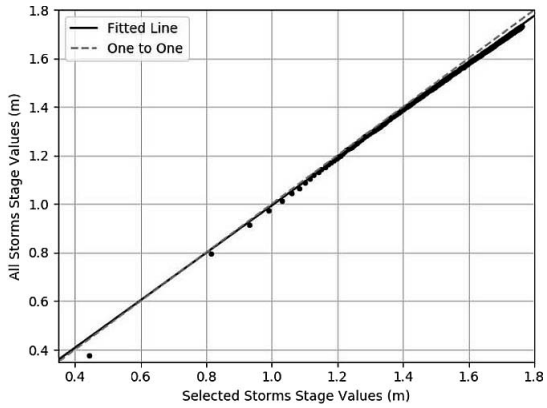

Figure 9. Scatter plot of stage values and the fitted line (solid). Additionally, a one-to-one line is shown (dash-dot). The stage values are nearly identical and follow the one-to-one line.

the timing of the storm events are identical and the tidal phasing is dependent on the time of storm events in the life cycle, the tidal contributions to stage are identical. Considering that the lower return interval years are associated with smaller surge values, the tides comprise a large percentage of the total stage. As a result, at the smaller return interval years, where the tidal contribution is dominant, the stage-frequency curves are nearly identical. Where the tidal contribution is not as significant and the storm surge plays a dominant role (high return interval years), the disparity between the representative and full storm suites is greater.

By isolating the tidal contribution from the total stage and considering only the storm surge, it can be seen in Figure 8 (red curves) that beyond return interval year 45, the standard deviation of the representative storm suite is slightly below that of the full storm suite. Although the standard deviation of the representative storm suite is less than that of the full storm suite, the magnitude remains relatively small (approximately 0.015 m).

The differences in both the average and the standard deviation of hazard distributions confirms that the methodology outlined in this paper for the selection of a representative storm suite in Monte Carlo life cycle modeling is technically justified.

Regression

The mean stage-frequency curve of both the representative and full storm suites were further compared by rank ordering the stage values and plotting them as a scatter plot (Figure 9). A linear regression was then applied with the stage value of the selected storms as the independent variable and the stage value of all storms as the dependent variable. Additionally, Figure 9 shows the regression line plotted through the data points. The regression results in a coefficient of 0.98 with an intercept close to zero. The r^2 for the regression was 0.99, with a 95% confidence interval from 0.973 to 0.982.

The results from the regression demonstrate that the mean stage values for the representative storms correspond almost exactly with those of the full storm suite. The representative storms do slightly overestimate the storm surge values, although the slight overestimation is attributed to a conservative selection of representative storms.

Additionally, at return interval years 25, 50, 75, 100, 125, 150, 175, and 200, the stage values corresponding to the representative and full storm suite distributions were ranked and plotted against each other in a scatter plot (Figure 10). In general, the two distributions of stage-frequency curves can be seen to share similar characteristics. The outlying upper stage-frequency curve in Figure 6b is apparent throughout Figure 10, although relative to the remaining points it is negligible. The eight plots of Figure 10 do not encompass all return interval years, but they do provide a sample of the similarities of the distributions at various return interval years. The plots between return interval years 25, 50, 75, 100, 125, 150, 175, and 200 will not differ considerably from those shown.

CONCLUSIONS

This paper introduces a methodology for identifying and selecting coastal storm events that are representative of the events contained within a probabilistic storm database. An example representative storm suite was developed for Crisfield, Maryland at CHS ADCIRC save point 6125. Of the available 1150 storms (1050 tropical and 100 extratropical), 445 storms were identified as storms of interest. The 445 storms of interest were further reduced to 32 representative storms that effectively characterize the probabilistic space.

By simulating 75 iterations of a 216-year life cycle, a storm suite containing the 445 storms of interest were compared with the representative storm suite containing only 32 storms. For each life cycle simulated, nonparametric hazard curves were generated (stage, surge, significant wave height), resulting in 75 unique curves for each storm suite. The mean stage, surge, and significant wave height curves were shown to compare favorably with maximum errors of 0.03, 0.05, and 0.02 m, respectively.

Additionally, the distributions of stage- and surge-frequency curves resulting from the full and representative storm suites were compared, and the standard deviation of the stage-frequency curves across the return interval space was shown to be nearly identical for the lower return interval years, diverging at higher return interval years. This trend was shown to be attributed to the tidal contribution to total stage.

Visual inspection of a scatter plot comparing the distribution of stage-frequency curves at return interval years 25, 50, 75, 100, 125, 150, 175, and 200 showed minor outliers. Although one to two outliers were present, the scatter plots show that the remaining distribution of stage-frequency curves compare favorably.

The results indicate that use of a representative storm suite developed through the methodology outlined in this paper returns nearly identical hazard curves as that of the full storm suite. This conclusion is drawn not only from the similarities between the average hazard curves, but also the similarities between the distributions of hazard curves. Overall, this comparison provides the technical justification for the use of a representative storm suite in Monte Carlo life cycle modeling.

Although there is no computational reduction for G2CRM by using a representative storm suite in lieu of the full

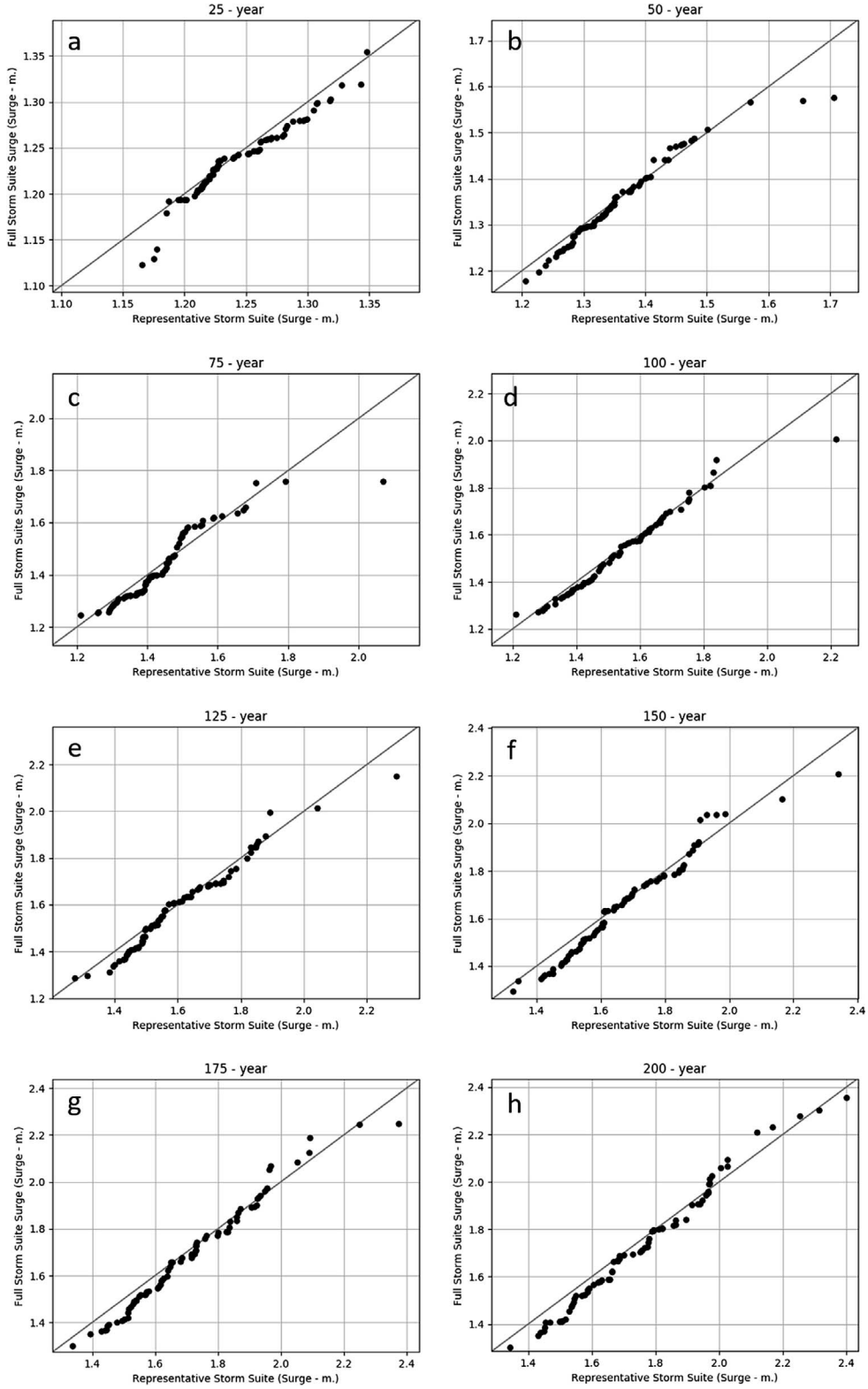

Figure 10. Scatter plot of representative and full storm suite stage-value distributions at return interval years (a) 25, (b) 50, (c) 75, (d) 100, (e) 125, (f) 150, (g) 175, and (h) 200. Two outlying points are apparent at return interval years 50, 75, 100, 125, and 150.

probabilistic storm suite, use of a representative storm suite is imperative for Beach-*fx* applications. Both Beach-*fx* and G2CRM employ the same storm selection methodology; therefore, although G2CRM was used to validate the representative storm suite, it can be concluded that the use of a representative storm suite is technically justifiable for both Beach-*fx* and other Monte Carlo life cycle models. In the context of Beach-fx, with upwards of 500 relevant storm events, 3.6–10.8 million profile response computations must be performed to represent the profile parameter space. Conversely, with a storm suite of 12–36 storm events, approximately 90,000–800,000 profile response computations are necessary to characterize the profile parameter space.

ACKNOWLEDGMENTS

The authors of this paper acknowledge the Coastal Hazards System (CHS) development team: Dr. Jeffrey Melby, Dr. Norberto Nadal-Caraballo, Victor Gonzales Nieves, and Fatimata Diop. Their feedback contributed to the authors' understanding of various attributes stored in the CHS. The authors additionally acknowledge the reviewers, as their comments significantly improved the presentation of this paper. This work was supported by the U.S. Army Corps Engineers Flood Risk Management Research Program.

LITERATURE CITED

Canick, M.R.; Carlozo, N., and Foster, D., 2016. *Maryland Coastal Resiliency Assessment*. Bethesda, Maryland: The Nature Conservancy, 107p.

Chouinard, L.E. and Liu, C., 1997. Model for recurrence rate of hurricanes in Gulf of Mexico. *Journal of Waterway, Port, Coastal, and Ocean Engineering,* 123(3), 113–119.

Cialone, M.A.; Massey, T.C.; Anderson, M.E.; Grzegorzewski, A.S.; Jensen, R.E.; Cialone, A.; Mark, D.J; Pevey, K.C.; Gunkel, B.L., and McAlpin, T.O., 2015. *North Atlantic Coast Comprehensive Study (NACCS) Coastal Storm Model Simulations; Waves and Water Levels*. Vicksburg, Mississippi: U.S. Army Engineer Research and Development Center, 252p.

Emanual, K., 2005. Increasing destructiveness of tropical cyclones over the past 30 years. *Nature*, 436, 686–688.

FEMA (Federal Emergency Management Agency), 2011. *Coastal Construction Manual: Principles and Practices of Planning, Siting, Designing, Constructing, and Maintaining Residential Buildings in Coastal Areas*, 4th edition. Washington, D.C.: FEMA, *P-55*, 251p.

Goldenberg, S.B.; Landsea, C.W.; Mestas-Nuñez, A.M., and Gray, W.M., 2001. The recent increase in Atlantic hurricane activity: Causes and implications. *Science*, 293(5529), 474–479.

Gravens, M.B.; Males, R.M., and Moser, D.A., 2007. Beach-fx: Monte Carlo life-cycle simulation model for estimating shore protection project evolution and cost benefit analyses. Washington, D.C.: American Shore & Beach Preservation Association [detached from *Shore & Beach*, 75(1), 12–19.

Hatzikyriakou, A.H. and Lin, N., 2017. Simulating storm surge waves for structural vulnerability estimation and flood hazard mapping. *Natural Hazards*, 89(2), 939–962.

Hatzikyriakou, A.H. and Lin, N., 2018. Assessing the vulnerability of structures and residential communities to storm surge: An analysis of flood impact during Hurricane Sandy. *Frontiers in Built Environment*, 4, 4p. doi:10.3389/fbuil.2018.00004

Irish, J.L. and Resio, D.T., 2013. Method for estimating future hurricane flood probabilities and associated uncertainty. *Journal of Waterway, Port, Coastal, and Ocean Engineering*, 139(2), 126–134.

Kossin, J.P.; Olander, T.L., and Knapp, K.R., 2013. Trend analysis with a new global record of tropical cyclone intensity. *Journal of Climate*, 26(24), 9960–9976.

Luettich, R.A.; Westerink, J.J., and Scheffner, N., 1992. *ADCIRC: An Advanced Three-Dimensional Circulation Model for Shelves, Coasts, and Estuaries, Report 1: Theory and Methodology of ADCIRC-2DDI and ADCIRC-3DL*. Washington, D.C.: Coastal Engineering Research Center, Engineer Research and Development Center, *Technical Report DRP-92-6*, 143p.

Massey, T.C.; Anderson, M.E.; Smith, J.M.; Gomez, J.M., and Jones, R., 2011. *STWAVE: Steady-State Spectral Wave Model. User's Manual for STWAVE, Version 6.0*. Vicksburg, Mississippi: U.S Army Engineer Research and Development Center, *ERDC/CHL TR-11-1*, 90p.

Melby, J.A.; Nadal-Caraballo, N.; Ratcliff, J.J.; Massey, T.C., and Jensen, R.E., 2017. *Sabine Pass to Galveston Bay Wave and Water Level Modeling*. Vicksburg, Mississippi: U.S. Army Engineer Research and Development Center, 287p.

Myers, V.A., 1970. *Joint Probability Method of Tide Frequency Analysis Applied to Atlantic City and Long Beach Island, N.J*. Silver Spring, Maryland: Office of Hydrology, Environmental Science Services Administration, U.S. Department of Commerce, *ESSA Technical Memorandum WBTM HYDRO 11*, 109p.

Nadal-Caraballo, N.C.; Melby, J.A., and Ebersole, B.A., 2012. *Statistical Analysis and Storm Sampling Approach for Lakes Michigan and St. Clair: Great Lakes Coastal Flood Study*. Vicksburg, Mississippi: U.S. Army Engineer Research and Development Center, *ERDC/CHL TR-12-19*, 156p.

Nadal-Caraballo, N.C.; Melby, J.A.; Gonzalez, V.M., and Cox, A.T., 2015. *Coastal Storm Hazards from Virginia to Maine*. Vicksburg, Mississippi: U.S. Army Engineer Research and Development Center, *ERDC/CHL TR-15-5*, 221p.

Nature Conservancy, 2018. *Coastal Resilience*. http://coastalresilience.org.

Rahmstorf, S., 2017. Rising hazard of storm-surge flooding. *Proceedings of the National Academy of Sciences of the United States of America*, 114(45), 11806–11808.

Resio, D.T., 2007. *White Paper on Estimating Hurricane Inundation Probabilities*. Vicksburg, Mississippi: U.S. Army Corps of Engineers Engineer Research and Development Center, 146p.

Resio, D.T.; Irish, J., and Cialone, M., 2009. A surge response function approach to coastal hazard assessment—Part 1: Basic concepts. *Natural Hazards,* 51(1), 163–182.

Scheffner, N.W.; Clausner, J.E.; Militello, A.; Borgman, L.E.; Edge, B.L., and Grace, P.J., 1999. *Use and Application of the Empirical Simulation Technique: User's Guide*. Vicksburg, Mississippi: U.S. Army Engineer Research and Development Center, *Technical Report CHL-99-21*, 193p.

Sobel, A.H.; Camargo, S.J.; Hall, T.M.; Lee, C.Y.; Tippett, M.K., and Wing, A.A., 2016. Human influence on tropical cyclone intensity. *Science,* 353(6296), 242–246.

Toro, G.R.; Niedoroda, A.W.; Reed, C.W., and Divoky, D., 2010a. Quadrature-based approach for the efficient evaluation of surge hazard. *Ocean Engineering,* 37(1), 114–124.

Toro, G.R.; Resio, D.T.; Divoky, D.; Niedoroda, A.W., and Reed, C., 2010b. Efficient joint-probability methods for hurricane surge frequency analysis. *Ocean Engineering,* 37(1), 125–134.

USACE (U.S. Army Corps of Engineers), 2018. *Coastal Hazards System*. https://chs.erdc.dren.mil.

USGS (U.S. Geological Survey), 2018. *Coastal Change Hazards Portal*. https://marine.usgs.gov/coastalchangehazardsportal/.

Walsh, K.J.; McBride, J.L.; Klotzbach, P.J.; Balachandran, S.; Camargo, S.J.; Holland, G.; Knutson, T.R.; Kossin, J.P.; Lee, T.C.; Sobel, A., and Sugi, M., 2016. Tropical cyclones and climate change. *WIREs Climate Change*, 7, 65–89. doi:10.1002/wcc.371

Webster, P.J.; Holland, G.J.; Curry, J.A., and Chang, H.R., 2005. Changes in tropical cyclone number, duration, and intensity in a warming environment. *Science,* 309(5742), 1844–1846.